J. Fluid Mech. (1984), *vol.* 149, *pp.* 101–125
Printed in Great Britain

Cellular patterns with boundary forcing

By S. ZALESKI

Groupe de Physique des Solides de l'École Normale Supérieure,
24 rue Lhomond, 75231 Paris CEDEX 05

(Received 20 December 1983)

In this paper we investigate some effects of a boundary forcing on 2-dimensional cellular patterns in instabilities above threshold. Boundary forcing is modelled as an inhomogeneous boundary condition on the slowly varying amplitude A, i.e. $A = \lambda e^{i\phi_0}$ on boundaries. The relevant range is $\lambda = O(\epsilon^{\frac{1}{2}})$, where ϵ is the relative distance to the linear-instability threshold. A wavenumber-selection mechanism then occurs, resulting in a band of selected wavenumbers of width proportional to λ. For large values of $\lambda\epsilon^{-\frac{1}{2}}$ it is shown that no stationary solution exists outside the band of Eckhaus-stable wavenumbers (Eckhaus 1965). For finite geometries of size L, a nonlinear analogue of 'quantization' of modes is investigated. The amplitude equation (equivalent to a space-dependent Ginzburg–Landau model) is analysed by an expansion in powers of $\exp(-L/\xi)$, where ξ is the coherence length. The range $\lambda = O(\epsilon)$ is also investigated. A correction to previous theories of wavenumber selection through boundaries (Cross, Daniels, Hohenberg & Siggia 1983*a*; Pomeau & Zaleski 1981) is calculated. The latter results are general and assume only the existence of a higher-order stationary amplitude equation, which is recast in a form consistent with its boundary conditions.

1. Introduction

The pattern of cellular structures above the linear-instability threshold has been the subject of a number of investigations. Cellular structures arise in some spatially periodic instabilities, of which the most studied one is the Rayleigh–Bénard thermoconvective instability. Centrifugal instability of Taylor–Couette flow is another example. For such instabilities, the laminar or purely conducting state of the fluid is unstable slightly above the instability threshold for a finite range of wavenumbers of width $\epsilon^{\frac{1}{2}}$, where ϵ is the small relative distance to threshold. The problem then arises of determining which wavevector will be observed. Moreover, one would like to know more precisely the perturbed velocity and/or temperature fields when nonlinear terms and lateral boundary conditions are fully taken into account. This problem for the case of perfectly parallel rolls or vortices has been extensively investigated. The flow is then two-dimensional and the perturbation fields depend only on two coordinates, the radial and axial coordinates r and z for Taylor–Couette flow, or a horizontal coordinate x and the vertical one z for Rayleigh–Bénard instability.

In the present work we investigate the case where some external effect generates lateral rolls and/or vortices, independently of the main instability mechanism in the bulk. This boundary forcing is a well-known feature in the Taylor–Couette problem. In the following we show that boundary forcing has two main effects: it broadens the extent of the selected wavenumbers, and increases the number of modes near threshold. These results might have been expected from previous results, but are new

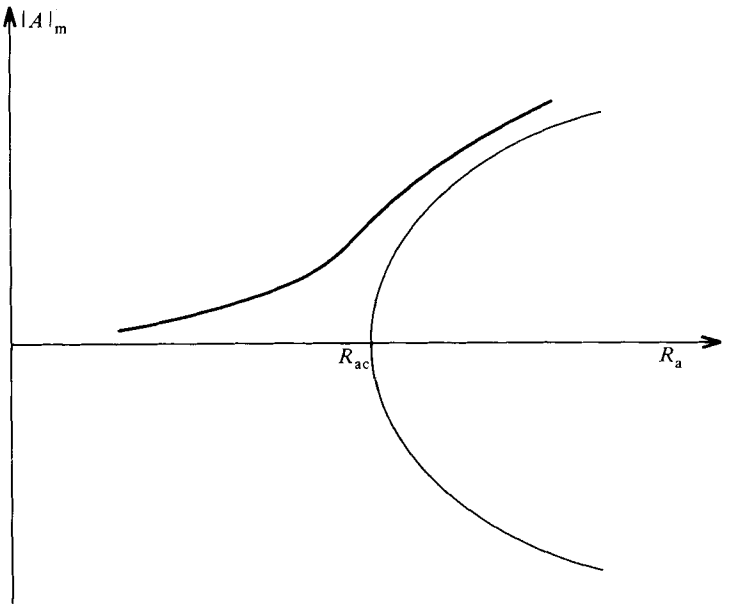

FIGURE 1. The imperfect bifurcation. The variation of the modulus of the slowly varying amplitude $|A|_m$ in the middle of the cell is plotted versus the control parameter R_a. In the perfect case (thin line) (e.g. $A = 0$ on boundaries) a sharp bifurcation occurs. It is replaced by a continuous increase of $|A|_m$ in the imperfect case (thick line).

for the range of parameters investigated. Moreover, the intuitive notion of 'quantization' of modes in a finite box is made more explicit through nonlinear calculation.

Experimental use of boundary forcing is rather widespread. In Taylor–Couette flow non-rotating endcaps produce vortices, which originate in the Ekman boundary layers on the walls. It was shown by Benjamin (1978*a*, *b*) and Mullin (1982) that such a configuration produces an 'imperfect' bifurcation near threshold: the end vortices exist for any Taylor number, and induce vortex motion in the bulk below the linear threshold (figure 1). For large aspect ratios a large multiplicity of modes is observed (Mullin 1982). Snyder (1969) investigated wavenumber selection existing near threshold in Taylor–Couette flow. He found that modes within a broad band of wavenumbers could be stable near threshold, apparently covering the whole band of wavenumbers that can be found stable when boundary conditions are accounted for.

In Rayleigh–Bénard convection various devices allow the forcing of convective motion. A heat flux can be imposed on the lateral boundaries, thus producing a destabilizing horizontal temperature gradient, and subcritical rolls. Such a condition was produced by Croquette & Pocheau (1983) with the help of a wire fixed on the lateral wall of the convective fluid layer. Subcritical convective motion was produced by Wesfreid, Berge & Dubois (1979). These latter authors conducted experiments where the lower plate of the cell was divided in several thermally independent parts maintained at different temperatures. Thus supercritical conditions could be produced on the extent of a pair of rolls near the lateral boundaries. This is equivalent to a boundary forcing when heating is subcritical in the remainder of the box. Finally Wesfreid & Croquette (1980) produced forced ascending flow in the bulk of the convection cell. This type of perturbation also induces rotation of nearby rolls.

Other features, like time-dependent heating or Rayleigh–Bénard convection between non-horizontal plates, can produce the equivalent of such forcing terms (Cross, Hohenberg & Lücke 1983). The problem of a heat flux through lateral boundaries was studied theoretically by Daniels (1977, 1978), Hall & Walton (1977) and Stewartson & Weinstein (1979). The effect of Ekman vortices on Taylor–Couette flow was also discussed by Walton (1980). This author considered the case of a small difference in the angular velocities of the concentric cylinders. However, the limit of large aspect ratio was not investigated in connection with the wavenumber-selection problem.

The effect of various boundary conditions on wavenumber selection was investigated recently (Cross *et al.* 1983*a*; Pomeau & Zaleski 1981; Potier Ferry 1983; Kramer & Hohenberg 1984; Zaleski 1984). When boundary conditions are not accounted for, the stability theory of Eckhaus (1965) and Kogelman & Di Prima (1970) predicts that a band of wavenumbers of extent $\epsilon^{\frac{1}{2}}$ will be stable above threshold (where ϵ is the relative distance to threshold). When homogeneous boundary conditions are taken, it was shown that the band of allowed wavenumbers is generally of width $O(\epsilon)$ (figure 3). Homogeneous boundary conditions can accommodate the complete vanishing of all perturbation fields, thus leading to a perfect bifurcation diagram; inhomogeneous boundary conditions, such as those exemplified in Appendix A, impose a non-zero value on the perturbation fields or their spatial derivatives. Wavenumber selection with inhomogeneous boundary conditions was investigated by Cross *et al.* (1983*a*) for the case where the magnitude of induced rolls on the boundary is small with respect to bulk roll motion. We are however interested in a different range of parameters, where the motion in the two regions is of comparable magnitude.

In the present work, we are interested in the phenomena occurring in the range of validity of the 'amplitude' expansion of Segel (1969) and Newell & Whitehead (1969). We suppose that the flow is strictly 2-dimensional (or azimuthal) and that it consists in an approximately periodic motion. As the flow is two-dimensional, the validity of the amplitude expansion is not hindered by large-scale-motion effects discussed by Siggia & Zippelius (1981).

2. The amplitude equation and its boundary conditions

Let x be the horizontal direction perpendicular to the roll axis and z the vertical direction. This 2-dimensional roll system can be described in terms of a rapidly varying temperature perturbation θ and a slowly varying amplitude A (figure 2). The latter is related to the former by

$$\theta(x,z) = \tfrac{1}{2}[A(x)\,f(z)\,\mathrm{e}^{\mathrm{i}q_c x} + \text{c.c.}] + O(\epsilon),$$

where c.c. stands for complex conjugate and f is a real function. $f(z)\,\mathrm{e}^{\mathrm{i}q_c x} + \text{c.c.}$ is the eigenmode of the linearized Oberbeck–Boussinesq equations at $R_a = R_{ac}$, with the appropriate boundary for $z = 0$, 1 and for an infinitely extended geometry in the x-direction (q_c is the critical wavenumber at onset).

The amplitude expansion (Segel 1969; Newell & Whitehead 1969; Graham & Domaradzki 1983) results in the following equation:

$$\tau_0 A_t = \epsilon A + \xi_0^2 A_{xx} - \frac{|A|^2 A}{A_0^2}, \tag{1}$$

where

$$A_{xx} = \frac{\partial^2 A}{\partial x^2}, \quad A_t = \frac{\partial A}{\partial t}.$$

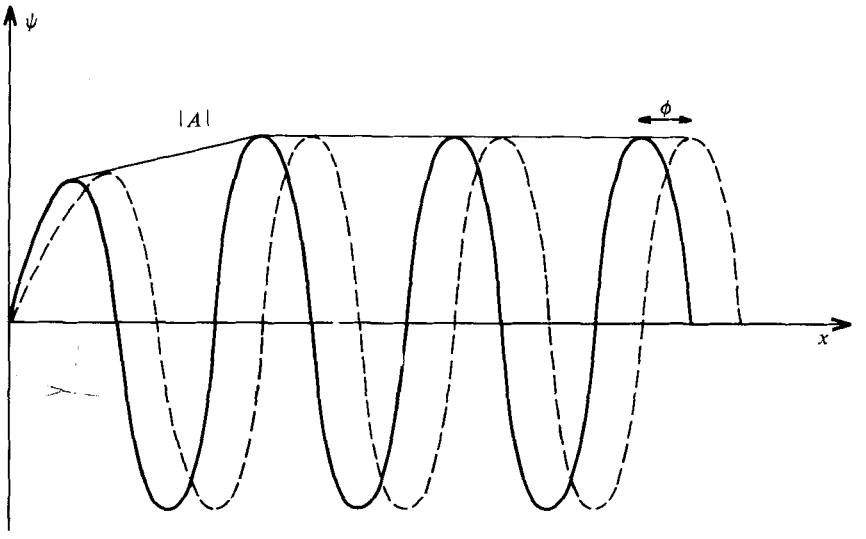

FIGURE 2. The slowly varying amplitude can be defined by its phase ϕ and its modulus $|A|$. The modulus (thin line) is the envelope of the rapidly varying perturbation, e.g. $\psi(x)$ (thick line). The phase can be represented by the difference with the phase of a rapidly varying perturbation of critical wavenumber (dotted line).

Equation (1) has been studied with various types of boundary conditions, which we shall discuss later. It can be put in a potential form

$$\tau_0 A_t = -\frac{\delta F}{\delta A},$$

where

$$F = -\frac{1}{2}\int\left(\epsilon|A|^2 - \xi_0^2|A_x|^2 - \frac{1}{2}\frac{|A|^4}{A_0^2}\right)\mathrm{d}x$$

and $\delta/\delta A$ is the Frechet (functional) derivative. F is the potential of the space-dependent Ginzburg–Landau model. This equation has been proposed for several cellular instabilities. Recently, Normand (1984) proposed a similar equation (with different nonlinear terms) for convection in high cylindrical containers. Pfister & Rehberg (1981) proposed to describe the wavy mode in Taylor vortex flow by (1). In this latter case only real amplitudes A were considered. (But it is possible to have a complex amplitude if its phase is to represent the phase of the wavy mode in the azimuthal direction at height x.)

A represents a slow modulation as

$$A = O(\epsilon^{\frac{1}{2}}), \quad A_x = O(\epsilon), \quad \text{etc.}$$

Solutions corresponding to a modulation of wavenumber $q = q_c + \delta$ are readily obtained:

$$A = A_0(\epsilon - \xi_0^2\delta^2)^{\frac{1}{2}}\exp\left[\mathrm{i}(\delta x + \phi_1)\right], \tag{2}$$

and the variation is again small:

$$|\delta| \leqslant \xi_0^{-1}\epsilon^{\frac{1}{2}}.$$

Thus a band of unstable wavenumbers of thickness of order $\epsilon^{\frac{1}{2}}$ is possible near threshold for steady patterns. The presence of homogeneous boundary conditions, i.e. $A = 0$, restricts the allowed band to $|\delta| = O(\epsilon\xi_0^{-1})$ (Pomeau & Zaleski 1981; Cross

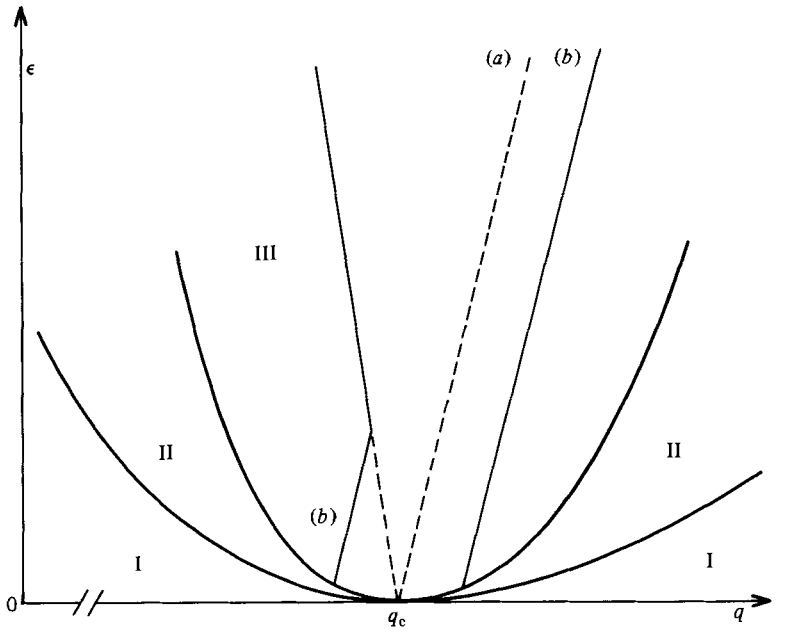

FIGURE 3. Various stability and existence analyses are summarized on this diagram. The relative distance ϵ to threshold is represented together with the wavenumber q of the solutions. In region I the laminar or conducting state is stable. In region II it is unstable, for wavenumbers in a band of extent $\epsilon^{\frac{1}{2}}$ around the critical one q_c. The roll system itself can be unstable with respect to the Eckhaus instability: stable rolls are restricted to region III. When boundary conditions are accounted for, and when the amplitude is correspondingly small on boundaries, the existing solutions (stable or unstable) are restricted to a band of extent $O(\epsilon)$, between lines (*a*). For inhomogeneous boundary conditions, i.e. $A(0) = \lambda e^{i\phi_0}$, this band is broadened (*b*). Near threshold, its extent is $\lambda/\sqrt{2}\,\xi_0 A_0$. Line (*b*) connects with the limit of Eckhaus-stable wavenumbers, which is shown to restrict further the band of solutions allowed by the boundaries. The width of the band is $O(\epsilon^{\frac{1}{2}})$. On the figure two orders of magnitude are represented: $\epsilon \approx \lambda$ and $\epsilon^{\frac{1}{2}} \approx \lambda$. Hence it only has a schematic character. The limits (*b*) for allowed wavenumbers are computed in Appendix B.

et al. 1983*a*). The exact computation of the bandwidth requires an amplitude equation at a higher order with respect to ϵ, as also shown in Appendix B. Various wavelength-selection results are plotted on figure 3.

The derivation of boundary conditions, when there is a small amount of forcing at the boundaries, is a rather tricky problem. It requires an asymptotic matching between two regions: a region of finite size near the lateral wall (or 'outer region') and the bulk region, or 'inner region' where the amplitude expansion holds. We describe this matching in Appendix A. A solution of the half-infinite linear problem is needed in the outer region. It is expanded in harmonic and exponentially decaying modes in the horizontal direction. In the inner region, we make the usual amplitude expansion. Such a matching was done by Daniels (1977) for convection with free boundary conditions on the upper and lower plane, and with imperfect thermal lateral boundary conditions. They arise when some heat is assumed to flow through the endwalls. The existence of orthogonality relationships between the modes involved in the 'outer' expansion greatly simplifies the derivation. Stewartson & Weinstein (1979) did similar computations for rigid horizontal and various lateral boundary conditions. Both papers derive the following boundary conditions:

$$A = \lambda e^{i\phi_0} \quad \text{on the boundaries,} \tag{3}$$

where λ, ϕ_0 are some constants which are to be computed from the exact physical boundary conditions on the sidewalls. In Appendix A we show how a similar boundary condition can be derived for the case of Boussinesq convection with rigid boundary conditions. The result should readily be extended to free horizontal boundary conditions or to other problems. The main assumption is that the amount of forcing, measured by λ, is small. We find

$$A + \xi_1 A_x + \xi_2 A_x^* = \lambda \, \mathrm{e}^{\mathrm{i}\phi_0} + O(\lambda^2).$$

While doing so, we use some non-trivial orthogonality relations between the linear modes of the 'rigid' case. Those relations simplify the derivation of the boundary conditions, but are much more intricate than in the 'free' case and were not employed in previous work.

For the Taylor–Couette problem the imperfection arises from the presence of rigid endcaps at the bottom (and sometimes at the top) of the fluid. Let u, v and w be the components of the velocity perturbations in the radial, azimuthal and vertical direction. (The amplitude expansion should now be made in the vertical direction.) The primary flow is the Couette flow, given by $U = W = 0$, $V = A'r + B'/r$, where r is the radial coordinate and A', B' some constants. In the case of non-rotating endcaps, the end boundary conditions are

$$u = w = 0, \quad v + V = 0 \quad \text{at } z = 0, L.$$

Starting from these conditions, a matching similar to the one of Appendix A can formally be done. However, this matching requires V to be small enough. Writing the 'outer' expansion is then equivalent to finding the Ekman vortices near the endcaps by a weakly nonlinear expansion. It is difficult to estimate the merit of this expansion as the inhomogeneous term in the boundary condition is now $O(1)$. Stewartson & Weinstein (1979), however, computed λ and ϕ_0 in (3) for various configurations of Taylor–Couette flow between concentric cylinders of almost equal angular velocity. Another approach is to compare (3) with the experimental findings. Snyder (1969) found that there was no variation of the size of the end vortices with the bulk wavenumber. This matches the fact that (3) fixes the phase at the boundary. Another experimental fact is that for Taylor–Couette flow the amplitude is larger at the boundaries than in the bulk. This gives a sufficient basis to retain (3) as a model of the actual experimental situation.

Half-infinite solutions can be obtained by considering only one boundary condition. A simple analysis of (1) (Cross *et al.* 1983*a*) in the case $\epsilon \ll \lambda \ll A_0 \epsilon^{\frac{1}{2}}$ shows that these solutions have their wavenumber still restricted to a small band:

$$|\delta| < \frac{\lambda}{\sqrt{2}\, \xi_0 A_0}.$$

For $\lambda = O(\epsilon^{\frac{1}{2}})$ the problem has not been studied to our knowledge. We first extend the analysis of half-infinite solutions to this latter case. Then we consider the bifurcation diagram for large L, that is $\lambda L / A_0 \xi_0 \gg 1$. Together with the assumption $\lambda = O(\epsilon^{\frac{1}{2}})$, this gives a somewhat different point of view compared to that of Cross *et al.* (1983*a*) and Daniels (1977, 1978) (allowing us to find new bifurcating branches in finite geometries). We also discuss the 'quantization' of the solution and locate the possible defects.

3. Half-infinite solutions

Let us consider a scaled version of (1). We define

$$\bar{A} = \frac{A}{A_0 \epsilon^{\frac{1}{2}}}, \quad \bar{x} = x\xi_0^{-1}\epsilon^{\frac{1}{2}}, \quad \bar{t} = \frac{t\epsilon}{\tau_0}.$$

It then follows that
$$\left.\begin{aligned} \bar{A}_{\bar{t}} &= \bar{A} + \bar{A}_{\bar{x}\bar{x}} - |\bar{A}|^2 \bar{A}, \\ \text{with the boundary condition} \quad \bar{A}(0) &= b\,\mathrm{e}^{\mathrm{i}\phi_0}, \end{aligned}\right\} \tag{4}$$

where $b = \lambda/A_0\epsilon^{\frac{1}{2}}$. Hereinafter, we omit the overbars for simplicity. We look for stationary solutions of (4) in the region $x > 0$. Two invariant quantities (i.e. independent of x) can be built from such a solution A of (1) if $A_t = 0$ (Newell & Whitehead 1969)

$$E = \tfrac{1}{2}|A|^2 - \tfrac{1}{4}|A|^4 + \tfrac{1}{2}|A_x|^2,$$
$$K = \tfrac{1}{2}\mathrm{i}(AA_x^* - A^*A_x),$$

where A^* denotes the complex conjugate of A. These quantities are invariants of the 'motion' with respect to the space variable x for a stationary solution:

$$\frac{\mathrm{d}E}{\mathrm{d}x} = 0, \quad \frac{\mathrm{d}K}{\mathrm{d}x} = 0.$$

They are connected to invariants of higher-order amplitude equations as shown in Appendix B and by Pomeau, Zaleski & Manneville (1983).

Consider now the modulus r and phase ϕ of A. Then

$$E = \tfrac{1}{2}r^2 - \tfrac{1}{4}r^4 + \tfrac{1}{2}r_x^2 + \frac{1}{2}\frac{K^2}{r^2}, \quad K = r^2\phi_x. \tag{5a,b}$$

The variation of r in the x-variable can be described as the motion of a particle of abscissa r and energy E in the potential $V_K(r)$ (figure 5):

$$E = \tfrac{1}{2}r_x^2 + V_K(r), \quad \text{with} \quad V_K(r) = \tfrac{1}{2}r^2 - \tfrac{1}{4}r^4 + \frac{1}{2}\frac{K^2}{r^2}.$$

We look for solutions that are periodic in the limit $x \to \infty$. For $K \neq 0$ solutions of (4) converge exponentially to periodic solutions:

$$A \xrightarrow[x\to\infty]{} (1-a^2)^{\frac{1}{2}}\,\mathrm{e}^{\mathrm{i}(ax+\phi_1)}. \tag{6}$$

The rapid modulation corresponding to these solutions has at infinity a wavenumber $q = q_c + \xi_0^{-1}\epsilon^{\frac{1}{2}}a$. For such a solution,

$$\phi_x \xrightarrow[x\to\infty]{} a, \quad r \xrightarrow[x\to\infty]{} (1-a^2)^{\frac{1}{2}},$$
$$2E = \tfrac{1}{2}(1-a^2)(1+3a^2), \quad K = (1-a^2)a.$$

On the boundary, let us define $c = r_x(0)$, then from (5a) and as $r(0) = b$:

$$K^2|_b = \tfrac{1}{2}b^2[b^4 - 2b^2 - 2c^2 + 4E]. \tag{7}$$

The wavenumber a is hence determined as a solution of a bicubic equation, once c is known:

$$(1-a^2)^2a^2 = \tfrac{1}{2}b^2[(1-b^2)^2 - 2c^2 + 2a^2 - 3a^4]. \tag{8}$$

The two sides of (8) are maximal for $a = 1/\sqrt{3}$. This is precisely the value at which solutions of the form (8) are marginal with respect to the well-known Eckhaus instability. This remark can be used for instance in a graphic reasoning which would consist in looking for intersections of the graphs of the two sides of (8). From such a reasoning $a = 1/\sqrt{3}$ is at least a double root of (8). This fact largely helps to compute and factorize the discriminant of (8).

We find (after some lengthy computations)

$$\Delta = -\tfrac{1}{8}c^2b^4[(b^2-\tfrac{2}{3})^3 - 2c^2b^2],$$

where Δ is the discriminant of the cubic equation for a^2, normalized as in Abramowitz & Stegun (1968). Purely imaginary roots of (8) must also be excluded. Such roots appear pairwise for values of the parameter yielding the root $a^2 = 0$. Substituting in (8) leaves

$$(1-b^2)^2 - 2c^2 = 0. \tag{9}$$

The meaning of this relation is discussed below.

We now discuss the possible solutions, depending on the value of b^2.

3.1. *Range* $0 \leqslant b^2 < \frac{2}{3}$

A single type of solution is possible for this range of b. It corresponds to solutions that have a limit value of A larger than b (i.e. $|A(\infty)| > |A(0)|$, see also figure 7*a*, *b*). They correspond to a motion in the potential V described as follows: it starts to the left of the relative maximum S of V and reaches S asymptotically as $x \to \infty$ (figure 5*b*). For $b^2 < \frac{2}{3}$ and $c \neq 0$, Δ is positive and there is only one pair of opposite roots $\pm a$ for (8). For fixed b there is hence a one-to-one correspondence between the parameters c and a.

Moreover, a increases with decreasing c. (This can be deduced for instance from the above-described graphic reasoning.) For $c = 0$ (8) is simply solvable. The roots are $a_1 = \pm b/\sqrt{2}$ and $a_2 = \pm(1-b^2)^{\frac{1}{2}}$. a_2 corresponds to a particle motionless at the fixed point Q (i.e. relative minimum of V). It corresponds to a solution likely to be unstable for $b^2 < \frac{2}{3}$ with respect to the Eckhaus instability. The root a_1 is the limiting value of the solutions for $c \neq 0$ and corresponds to the trajectories from P to S. This implies that for $b^2 < \frac{2}{3}$ we recover the condition $|a| < b/\sqrt{2}$, that is

$$|\delta| < \frac{\lambda}{\sqrt{2}\,\xi_0 A_0}. \tag{10}$$

Thus for sufficiently large λ there is a band of selected wavenumber larger than the $O(\epsilon)$ band expected for $\lambda = 0$. This result is proved here for the case $\lambda = O(\epsilon^{\frac{1}{2}})$.

This type of solution matches with the solutions lying in the previously computed bands for $b = \lambda\epsilon^{-\frac{1}{2}}A_0^{-1} \to 0$. For $\lambda = O(\epsilon)$ the $O(\epsilon)$ band can again be computed, as shown in Appendix B. The various allowed bands are summarized in figure 3.

3.2. *Range* $\frac{2}{3} < b^2 < 1$

The previous type of solutions still exists, but solutions with $|A(\infty)| < |A(0)|$ appear. They correspond to a motion in the potential V starting from a point T and reaching asymptotically the maximum S (figures 5*b*, 6*a*). When solving (8) to find such solutions, one has to eliminate spurious solutions of a particular type: they correspond to a motion starting from T with enough energy to reach the fixed point Q, which, however, is separated from T by a potential barrier. The solutions a of (8) now span the whole Eckhaus-stable band. For $c = 0$ the corresponding solution is a

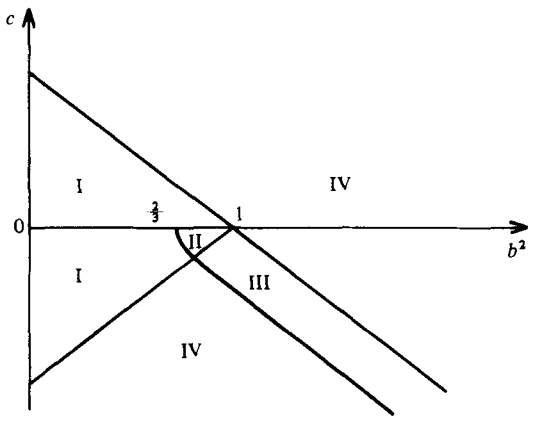

FIGURE 4. The set of allowed values for $c = r_x(0)$ is plotted versus $b^2 = |A(0)|^2$. For small b there is a single solution of (8) in region I. In region II two solutions are possible, in region III there is again only one solution. No solutions exist in region IV. The shape and wavenumber of the various solutions are discussed in the text.

constant with $a = a_2$ as defined above. It corresponds to a particle motionless at S on figure 5.

3.3. *Range* $b^2 > 1$

For this range the solutions described in §3.1 disappear. There is again a one-to-one correspondence between c and a, with a varying in the whole band of Eckhaus-stable wavenumbers.

3.4. *Summary of results and singular behaviours*

The possible occurrence of various solutions has been represented on figure 4. The number of solutions is determined from the value of the discriminant Δ, and from the elimination of spurious solutions. Some of those, with $a^2 < 0$, are located with the help of (9). They correspond to an exponential decay of A in the x-direction. Others are described in §3.2. Finally $|A(\infty)| < |A(0)|$ requires $c < 0$. Four regions in figure 4 result. In region II, 2 roots of (8) are retained, whereas in region I and III only one has a physical meaning. In region IV there is no solution.

Several singular behaviours can be distinguished in the diagram of figure 4. On the lower boundary of regions II and III solutions appear marginally as LN trajectories in figure 5*a*. They converge algebraically to a marginally stable periodic pattern in the bulk. For $b^2 = \frac{2}{3}$ and $c = 0$, $a = 1/\sqrt{3}$ is a triple root of (8). This latter solution should be worth further study, as its stability properties in finite length should also be very singular. These last two types of solutions can be expected to be marginally stable, as also appears from the analysis of the finite-length problem.

To summarize our results, we have studied the various possible solutions and wavenumbers with respect to the boundary value $b = |A(0)|$. We related the wavenumber to the free parameter $c = r_x(0)$. This free parameter will be fixed when a second boundary is added. A finite number of solutions is then possible, through a 'quantization' condition of a sort that we shall study below.

4. Bifurcation of finite-length solutions

We now proceed to the study of stationary solutions of (3) with the boundary conditions:

$$A(\pm l) = b\,\mathrm{e}^{\mathrm{i}\phi_\pm}, \tag{11}$$

with $b = \lambda/A_0\,\epsilon^{\frac{1}{2}}$ and $l = L/\xi$ and where $\xi = \xi_0\,\epsilon^{-\frac{1}{2}}$ is the coherence length, $2L$ is the length of the domain and λ is the modulus of the amplitude at the boundaries in the original equation. $\phi_\pm$ is the phase on the boundaries. It is defined relatively to the phase of the periodic solution of critical wavenumber q_c (figure 2) and hence depends on the length L (see Appendix A, (A 23)). Solutions of (4) can be written as the inverse of simple elliptic integrals: the abscissa $x(r)$ corresponding to a modulus r of the amplitude can be extracted from $(5a,b)$, and a similar operation gives the phase. In the simple case where r varies monotonically between its minimum value r_m and its end values, one has

$$x(r) - x(r_m) = \pm \int_{r_m}^{r} \frac{\mathrm{d}r}{(2E - V_K(r))^{\frac{1}{2}}}, \tag{12a}$$

$$\phi(r) - \phi(r_m) = \int_{r_m}^{r} \frac{K\,\mathrm{d}r}{r^2(2E - V_K(r))^{\frac{1}{2}}}. \tag{12b}$$

$r(x)$ and $\phi(x)$ can hence be expressed with the help of elliptic functions, by inversion of $(12a,b)$. The conditions (11) are then equivalent to the constraints arising from the boundary conditions

$$l = \int_{r_m}^{b} \frac{\mathrm{d}r}{(2E - V_K)^{\frac{1}{2}}}, \quad \Delta\phi = \int_{r_m}^{b} \frac{K\,\mathrm{d}r}{r^2(2E - V_K)^{\frac{1}{2}}}, \tag{13a,b}$$

where $\Delta\phi = \frac{1}{2}(\phi_+ - \phi_-)$. Thus the parameters E and K, which define the solutions, are related to l and $\Delta\phi$, which are given by (11). To find solutions of this implicit system, we first expand the integrals $(13a,b)$ in the limit of large l. We then present numerical computations of solutions of the system $(13a,b)$ for finite and small l. In the following, analytical expansions were made only in the simple case where $(12a)$ holds (i.e. with only one oscillation of r in the bulk). There should be no difficulty, however, in extending them to the general case. The contribution of additional oscillations is readily deduced from computations of Appendix C.

4.1. *Analytical expansion for large l*

Taking a large value of l (i.e. $L \gg \xi$) implies that the solution is close to two half-infinite ones glued together. Then for most solutions one has $K < K_{\text{Eckhaus}} = 2/3\sqrt{3}$, and we can parametrize the solutions by an approximate wavenumber a. Let $K = (1-a^2)a$ (a is exponentially close to the wavenumber of central rolls) and $E = \frac{1}{2}(1-a^2)(1+3a^2) + \eta$. We further restrict the expansion to the case $b^2 > 1-a^2$. The sign of η then distinguishes two types of solution. For $\eta < 0$ we recover the usual pattern of the solutions of the amplitude equation, with a perfectly regular shape (figure $6a$). For $\eta > 0$ the trajectory enters the region $PQRS$ in figure $5(b)$. In this region, the modulus of A is smaller than in the surrounding quasiperiodic regions (figure $5b$, $6b,c$). This corresponds to almost-stagnant fluid in a hydrodynamic instability, i.e. a region where roll motion is strongly damped. In Appendix C we expand integrals $(13a,b)$ analytically, with respect to the small parameter $\eta = \exp(-l)$. Similar expansions would give approximate solutions of (4) through computation of $(12a,b)$.

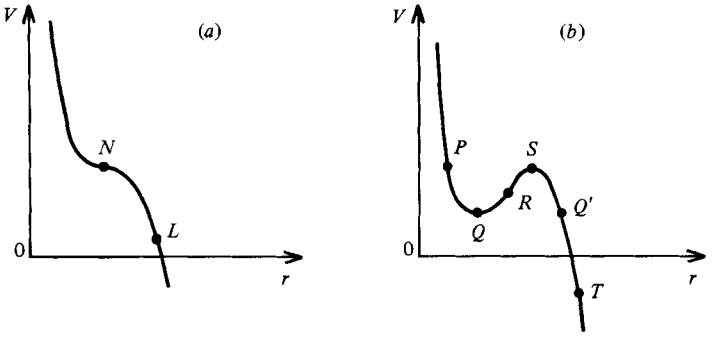

FIGURE 5. The potential V defined in text is plotted as a function of the modulus $r = |A|$. The solutions $r(x)$ for a given value of the invariant K can be represented as motions in this potential. (*a*) Marginal case: there is only one equilibrium point which corresponds to marginal stability of $A(x)$. (*b*) Generic case: the equilibrium point S corresponds to stable solutions and point Q to unstable ones. Trajectories in this potential are described in the text.

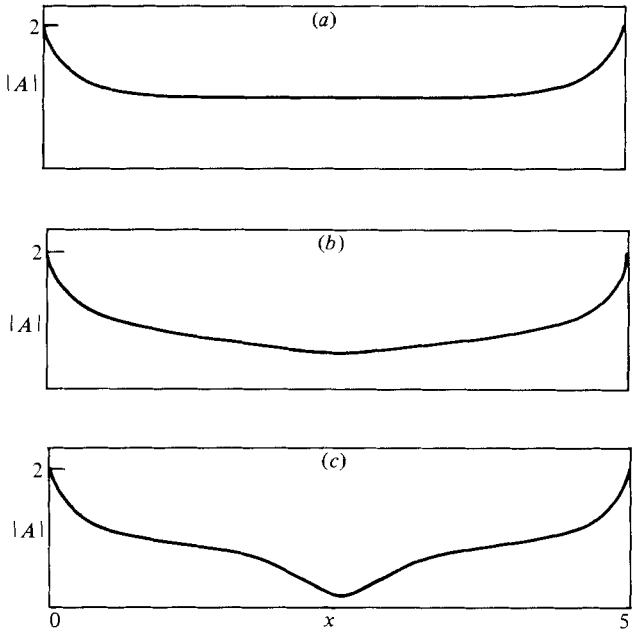

FIGURE 6. The modulus $r(x)$ of stationary solutions of (4). The dimensionless amplitude on boundaries is $b = 2$. (*a*) $\Delta\phi = 0$. (*b*) $\Delta\phi = 2$. For larger $\Delta\phi$, the solution sinks in the bulk until it reaches zero in the centre. (*c*) A 'kinked' solution; such a solution is unstable. All solutions were drawn using numerical solutions of (13*a*, *b*).

In Appendix C we show, at first order,

$$|\eta| = \frac{2\alpha^2}{(1-a^2)^2} e^{-l\alpha m_\pm}, \quad \text{where } \alpha = 2^{-\frac{1}{2}}(1-3a^2),$$

and

$$\Delta\phi = al + I(a, b, \eta), \tag{14}$$

with

$$I(a, b, \eta) \to I_\pm(a, b) = m_\pm \arctan \frac{1-3a^2}{a\sqrt{2}} - \arctan \frac{b^2-2a^2}{a\sqrt{2}},$$

(for $\eta \to 0_\pm$),

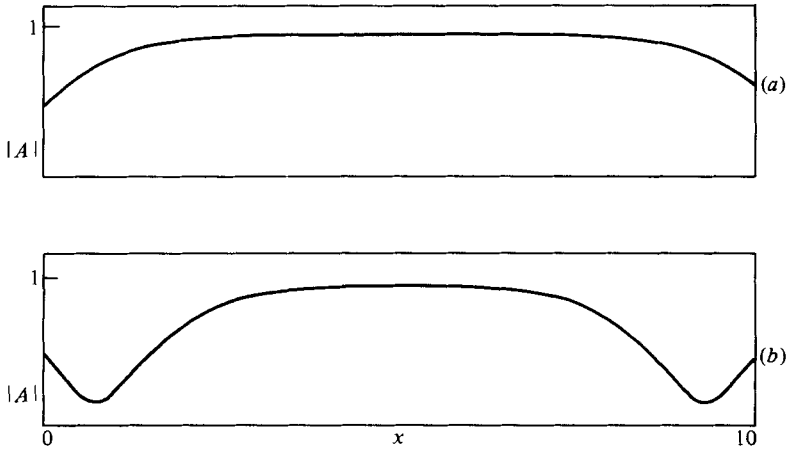

FIGURE 7. Various symmetric solutions without 'kinks' in the bulk are plotted as obtained, for $b < 1$, by a numerical shooting method. In all cases $b \approx 0.5$.

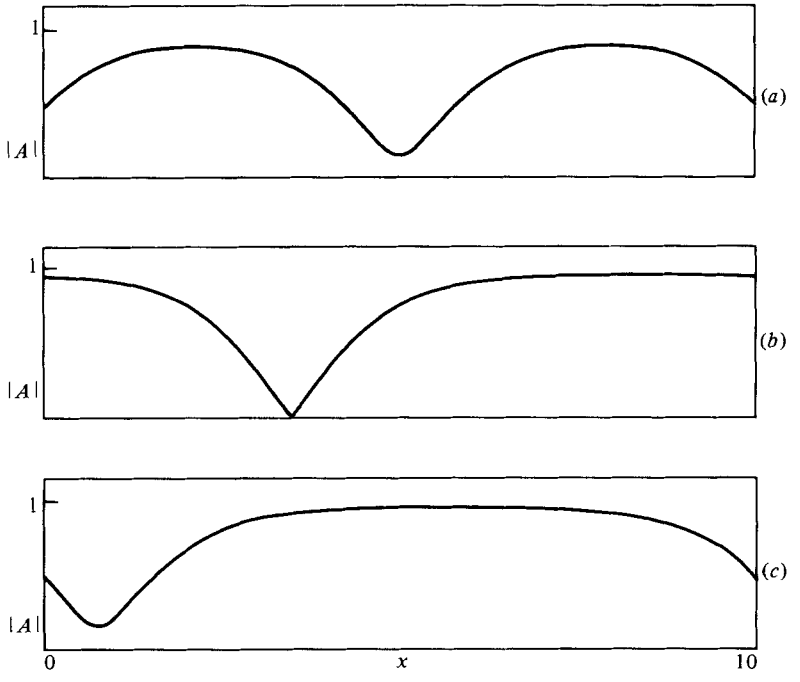

FIGURE 8. Other types of solution for $b < 1$: (*a*) $b = 0.5$: a symmetric 'kinked' solution can be found to evolve from that in figure 6(*c*). (*b*) $b = 0.985$: for $b \approx 1$, it can also evolve to an asymmetric solution. (*c*) $b = 0.5$: for lower b the kink is located at boundaries. All figures are drawn from numerical solutions obtained by the shooting method.

where $m_- = 1$ and $m_+ = 2$. The first term on the right-hand side of (14) is the bulk phase winding of periodic patterns with wavenumber a. $I(a, b, \eta)$ represents the phase gained or lost in the boundary layers at the ends and/or in the centre. Figure 9(*a*) represents a as a function of this phase adjustment $I_{\pm}(a, b)$. In an experiment, one would get a by a measurement of the bulk wavenumber and $\Delta\phi$ by measuring the overall number of oscillations, including the end ones.

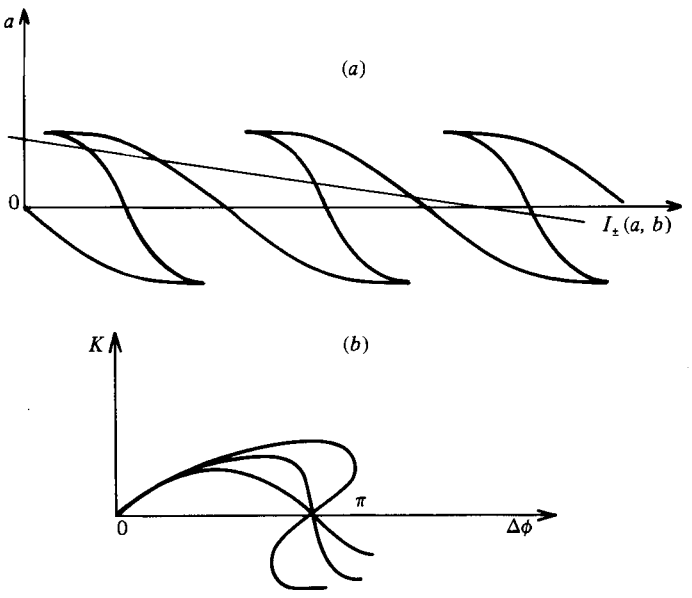

FIGURE 9. Resolution of (13a, b) (a) For large l an analytic expansion is made. The wavenumber a is related to $I_\pm(a, b)$. I_- corresponds to short branches in the wavy pattern and I_+ to long ones. For $\Delta\phi$ and l fixed the solutions lie at the crossing of the straight line $I_\pm = \Delta\phi - la$ and of the branches $(a, I_\pm)$. 'Kinked' solutions, corresponding to $I = I_+$ and unkinked ($I = I_-$) ones can thus be numbered. Numerical computations of $I(a, b, \eta)$ agree with analytical results very accurately: for $l > 5$, points calculated numerically and analytically coincide on the figure. (b) For smaller l, $\Delta\phi$ was related numerically to K: for fixed b and l, solutions lie on a curve in the $(\Delta\phi, K)$-plane. Several such curves are represented for different values of l. When l is small there is only one solution for fixed $\Delta\phi$. When l increases, new solutions appear as the curve is folding.

The set of solutions of (4) is best understood by means of a graphic resolution (figure 9a). It shows that the number of solutions grows like

$$n = \frac{2l}{\pi\sqrt{3}} = \frac{2L}{\pi\sqrt{3}\,\xi_0}\epsilon^{\frac{1}{2}}$$

and that solutions with $\eta > 0$ and $\eta < 0$ appear simultaneously. They hence have opposite stabilities. As there is an odd number of solutions with $\eta < 0$, and an even number of solution with $\eta > 0$, topological degree theory implies that the former are stable and the latter unstable. Thus 'kinks' or 'defects' in the bulk are unstable. In what follows, we investigate the immediate vicinity of the threshold and find a stable 'kinked' solution in a particular case.

4.2. *Numerical computations*

To find solutions in the limit $\epsilon \to 0$, i.e. $l \to 0$ and $b \to \infty$, we performed numerical computations of the integrals (13a, b). For each value of $\Delta\phi$ we find one or several possible values of the parameters E, K and r_m (b and l being held fixed). The solutions can be conveniently parametrized by K. To understand the meaning of this parameter, consider (5b): K has the form of an angular momentum and represents the rapidity of the phase change (it varies monotonically with a for $|a| \leqslant 1/\sqrt{3}$, so that a connection with previous results can easily be made). Close to the threshold, boundary layers have a thickness ξ of order $\epsilon^{-\frac{1}{2}}$, as is well known from theory and

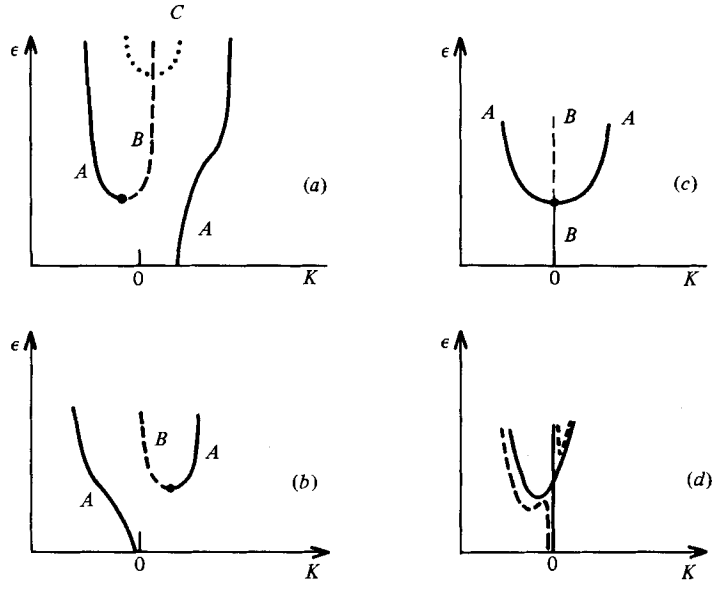

FIGURE 10. The bifurcation diagrams near $\epsilon = \xi_0^2 L^{-2}$. The invariant K is chosen for parametrization as it measures the rapidity of phase change (see text). (For lower l the whole interval is invaded by boundary layers. Hence it does not make sense to consider the bulk 'wavenumber' of the solutions.) (*a*) The first mode has N oscillations (branch A). For larger ϵ a solution with $N+2$ modes bifurcates (branch B). For even larger ϵ, i.e. for $b < 1$, new solutions appear (figure 7 and 8) (branch C). (*b*) When L is larger the first mode has $N+2$ oscillations. (*c*) For a definite value of L, the first mode is 'kinked' (branch B). It bifurcates into solutions of N and $N+2$ modes (branch A). (*d*) In experiments (Mullin 1982) the bifurcation of figure 10(*c*) is subcritical (full line). This lack of symmetry could be recovered if higher-order terms were kept in the amplitude expansion. Thus bifurcation diagrams (*a*, *b*) would also be modified (dotted line).

experiments (Wesfreid *et al.* 1978). For K not too large the solution consists of two boundary layers, r behaving like (in dimensionless units)

$$r = \frac{1}{x + l + b^{-1}}. \tag{15}$$

This was already stressed by Graham & Domaradzki (1983). However, these authors neglected the b^{-1} term, which is indeed small near threshold.

The result of these computations was represented as a family of curves in the $(K, \Delta\phi)$-plane (figure 9*b*). Each curve is drawn for a fixed value of l and b. Each point on the curve corresponds to a possible solution of system (13*a*, *b*). For small and large b, there is only one value of K for each $\Delta\phi$. When l or b exceeds some critical value, there is a folding of the curve around the value $\Delta\phi = \pi$, and a pair of new solutions appears (figure 9*b*). The bifurcation diagrams can be easily deduced, for various values of $\Delta\phi$.

For most values of $\Delta\phi$ the bifurcation is of the 'imperfect' type (figure 1). The 'secondary modes' correspond to those theoretically investigated by Schaeffer (1980) and observed by Mullin (1982). 'Secondary modes' are modes that do not bifurcate continuously from the basic solution existing for $\epsilon < 0$. They can be attained by first-order transitions (jumps) from other modes.

The bifurcation diagrams (figure 10) involve modes with N and $N+2$ waves. (For the sake of simplicity we have not represented the other possible secondary modes.) When L increases, $\Delta\phi$ varies proportionally and all modes are shifted to the left of figure 10. For $\Delta\phi = \pi$ a perfect bifurcation is recovered. For $\Delta\phi \neq \pi$ the first mode

in figure 10 has a shape depending on $\Delta\phi$. In most cases this shape is intermediate between shapes 'with' or 'without' defect.

For $\Delta\phi = \pi$ the first mode, existing at low values of ϵ, is a 'kinked' mode with $K = 0$, and its amplitude goes to zero somewhere in the bulk. The kinked region is a remainder of the zero-amplitude region that exists for $\epsilon < 0$ outside the subcritical boundary layers. Such solutions have indeed been observed by Mullin (1982).

However, our results differ from these observations in that we find no hysteresis. Indeed, hysteresis would result in an S-shaped bifurcation curve for the primary mode (figure 10*d*). As shown on this figure, this hysteretic behaviour breaks the symmetry between the N and $N+2$ modes. A simple argument shows that this behaviour cannot be deduced in the framework of the amplitude equation at lowest order. At this order the equations are symmetric with respect to the $K \to -K$, $\phi \to -\phi$ transformation, i.e. the bifurcation diagrams of figure 6(*a*) must be perfectly symmetric. This symmetry is linked to the symmetry with respect to the addition or subtraction of a wave, i.e. with respect to the transformation $\delta \to -\delta$ in (2). Only higher-order terms in the amplitude expansion can break this symmetry.

4.3. *Behaviour at larger values of* ϵ

As already implied in §2, new solutions appear when $b = (1-a^2)^{\frac{1}{2}}$. In dimensionalized variables this latter relation is equivalent to

$$\lambda = A_0(\epsilon - \xi_0^2 \delta^2)^{\frac{1}{2}}.$$

For $\epsilon \geqslant 3\lambda^2/2A_0^2$ all solutions have the boundary layers depicted in figures 7–8. Several oscillations are now possible in the *PQRS* region of figure 5(*b*), and a large variety of new solutions bifurcates. It is now possible that the kink previously located in the centre migrates to the ends (figures 8*b*, *c*). As b decreases, the kink is rapidly locked at a boundary. Such solutions are represented on the bifurcation diagram of figure 10(*a*). Their stability cannot be determined in a simple way. However, they are likely to be unstable, as in the limit $\lambda = 0$ asymmetric solutions were shown to be unstable (Pomeau & Zaleski 1981; Daniels 1981). Solutions with more oscillations in the *PQRS* region also appear, and their linear stability again probably depends on their more or less symmetric character. Such a symmetric pattern is represented in figure 8(*a*).

5. Conclusion

In conclusion we have observed some rather surprising features of the one-dimensional patterns, described by the amplitude equations near threshold. Although for half-infinite solutions the band of selected wavenumbers expands in a very simple way to reach the Eckhaus-instability limit, the bifurcation of finite-length solutions appears rather intricate. For large L/ξ all existing stationary solutions are contained in the band of Eckhaus-stable periodic states. For smaller L, however, comparison with periodic solutions loses its meaning, and stable solutions with 'kinks' in the amplitude can be found. The existence of such solutions precisely allows us to match the phase throughout the domain. It is expected that such 'kinks' could be found in other situations where such a matching is necessary. Such solutions have been found in the experimental study of the buckling of thin elastic plates (Boucif, Wesfreid & Guyon, 1983 and private communication). They have also been observed in numerical simulations of asymmetric roll systems, where a phase matching is also necessary (Pomeau & Manneville, private communication).

The effect of boundary conditions on mode selection is related to various other

effects in hydrodynamic instabilities. An important feature is the long time of relaxation to an equilibrium state. As shown in this paper, a marginally stable state can be approached in at least two ways: by forcing the system to get close to Eckhaus-unstable modes, or by getting close to the bifurcation point of figure 10(*d*). In such situations the relaxation time might diverge or at least be far greater than the characteristic diffusion time across the cell, i.e. $L^2\tau_0/\xi_0$.

The author wishes to thank Y. Pomeau for suggesting to him the subject of this paper and for many helpful discussions. The author also benefited from many discussions with P. Manneville and J. E. Wesfreid. Part of this work was realized while the author was visiting the Department of Astronomy of Columbia University, with support from grant NSF Phy 80-23721, and also while the author was visiting the Laboratoire d'Hydrodynamique et de Mécanique Physique, Paris, with support from the DRET.

Appendix A. Inhomogeneous boundary conditions for the slowly varying amplitude

The boundary conditions for the slowly varying amplitude are connected in this appendix to the original two-dimensional flow equations. We specifically consider the Rayleigh–Bénard problem with solid (no-slip) boundary conditions. In what follows, we describe a matching between the bulk region of the convective layer, where the amplitude expansion holds, or 'inner region', and a region of finite size near the end walls, or 'outer region'.

A.1. *The Oberbeck–Boussinesq equations*

The basic equations for stationary convection in the Boussinesq approximation can be reduced to the form

$$\boldsymbol{L}\boldsymbol{U} = \mathbf{N}(\boldsymbol{U}, \boldsymbol{U}), \tag{A 1}$$

where $\boldsymbol{U}$ is a vector of components $(u, w, \theta, -p)$, $\boldsymbol{L}$ is the operator

$$\boldsymbol{L} = \begin{pmatrix} \Delta & 0 & 0 & \partial_x \\ 0 & \Delta & R_\xi^{\frac{1}{2}} & \partial_z \\ 0 & R_a^{\frac{1}{2}} & \Delta & 0 \\ \partial_x & \partial_z & 0 & 0 \end{pmatrix},$$

and

$$\mathbf{N}(\boldsymbol{U}, \boldsymbol{U}') = \begin{pmatrix} -uu'_x - wu_z \\ -uw'_z - ww'_z \\ -u\theta'_x - w\theta'_z \\ 0 \end{pmatrix}.$$

The rigid boundary conditions are

$$u = w = \theta = 0 \quad \text{for } z = -\tfrac{1}{2}, \tfrac{1}{2}. \tag{A 2}$$

u and w are the horizontal and vertical components of the velocity field, θ is the temperature perturbation and p is the pressure. R_a is the Rayleigh number. Boundary conditions on the lateral wall must come from an analysis of the heat equation in the endwalls. We somewhat simplify the problem by assuming a constant heat flux of small amplitude through a thin insulating rigid wall:

$$u = w = 0, \quad \theta_x = \lambda_1 h(z) \quad \text{at } x = 0, L; \tag{A 3}$$

here $\lambda_1 h(z)$ is some externally controlled heat flux. We take $h(\frac{1}{2}) = h(-\frac{1}{2}) = 0$ for

consistency, and $h = O(1)$. λ_1 is a small scaling parameter. We assume h is smooth enough so that (A 1)–(A 3) has smooth solutions.

A.2. *Expansion of the outer solutions of the linear problem*

We consider now the linearized problem

$$\boldsymbol{L}\boldsymbol{U} = \boldsymbol{0} \tag{A 4}$$

with boundary conditions (A 2), and expand solutions in the form

$$\boldsymbol{U}(x, z) = \sum_{n=0}^{\infty} \beta_n \boldsymbol{U}_n(z)\, \mathrm{e}^{k_n x} + \text{c.c.}, \tag{A 5}$$

where k_n, β_n are real or complex numbers, $\boldsymbol{U}_n(z)$ are complex vector fields and c.c. stands for complex conjugate. The corresponding temperature perturbation and vertical velocity fields, chosen to have even symmetry in z, are of the form

$$\theta = \Big(\sum_{i=1}^{3} a_i \cosh p_i z\Big)\mathrm{e}^{kx},$$

$$w = -R_{\mathrm{a}}^{-\frac{1}{2}}\Big(\sum_{i=1}^{3} a_i (p_i^2 + k^2)^{-1} \cosh p_i z\Big)\mathrm{e}^{kx},$$

where $(k^2+p^2)^3 - R_{\mathrm{a}} k^2 = 0$. The above expressions can satisfy the horizontal boundary conditions (A 2) only for a discrete set of values of k. Stewartson & Weinstein (1979) (hereinafter referred to as SW) computed the k_n and the above eigenvalues up to $n = 10$, as well as their asymptotic forms for large n. For our approach it is useful to relate the $\boldsymbol{U}_n$ to a 1-dimensional eigenvalue problem. Consider vector fields on $(-\frac{1}{2}, \frac{1}{2})$:

$$\boldsymbol{F}_n(z) = \begin{pmatrix} f_{n1}(z) \\ f_{n2}(z) \\ f_{n3}(z) \end{pmatrix}, \tag{A 6}$$

where the components are arbitrary functions of z on the interval $(-\frac{1}{2}, \frac{1}{2})$. The k_n are related to eigenvalues of the problems

$$\boldsymbol{M}_{R_{\mathrm{a}}} \boldsymbol{F}_n = k_n^2 \boldsymbol{F}_n, \quad \boldsymbol{M}_{R_{\mathrm{a}}} \boldsymbol{F}_n^* = k_n^{*2} \boldsymbol{F}_n^*, \tag{A 7}$$

where k_n^* is the c.c. of k_n, and

$$\boldsymbol{M}_{R_{\mathrm{a}}} = \begin{pmatrix} 0 & 1 & 0 \\ 0 & 0 & 1 \\ -\mathrm{D}^6 & -3\mathrm{D}^4 + R_{\mathrm{a}} & -3\mathrm{D}^2 \end{pmatrix}$$

with $\mathrm{D} = \mathrm{d}/\mathrm{d}z$, and the boundary conditions

$$f_{ni} = f_{ni,z}^2 = 0 \quad \text{for } 1 \leqslant i \leqslant 3, \quad f_{ni,z}^3 + f_{ni+1,z} = 0 \quad \text{for} \quad 1 \leqslant i \leqslant 2. \tag{A 8}$$

We also define a Hermitian product for vector fields of the form (A 6):

$$(\boldsymbol{F}|\boldsymbol{G}) = \sum_{i=1}^{3} \int_{-\frac{1}{2}}^{\frac{1}{2}} f_i^*(z)\, g_i(z)\, \mathrm{d}z. \tag{A 9}$$

A pseudoadjoint operator can be defined for this product,

$$\boldsymbol{M}^{+}_{R_a} = \begin{pmatrix} 0 & 0 & -\mathrm{D}^6 \\ 1 & 0 & -3\mathrm{D}^4 + R_a \\ 0 & 1 & -3\mathrm{D}^2 \end{pmatrix},$$

and the adjoint problem reads

$$\boldsymbol{M}^{+}_{R_a} \boldsymbol{F}^{+}_n = k'^2_n \boldsymbol{F}^{+}_n$$

with the boundary conditions

$$\left.\begin{aligned} f^{+}_{ni} &= 0 \quad \text{for } 0 \leqslant i \leqslant 3, \\ \mathrm{D}f^{+}_{n3} &= \mathrm{D}^2 f^{+}_{n3} = \mathrm{D}^4 f^{+}_{n3} = 0 \end{aligned}\right\} \quad \text{at } z = \pm\tfrac{1}{2}.$$

We now assume that the $\boldsymbol{F}_n$ are a basis for the Hilbert space of fields (A 6) with products (A 9). Then we can identify $k_n = k'^*_n$, and we have the orthogonality relations

$$(\boldsymbol{F}^{+}_n | \boldsymbol{F}_m) = \delta_{nm} \tag{A 10}$$

for normalized eigenvectors.

The solutions of the auxiliary problem (A 6)–(A 8) are related to (A 5) by

$$\boldsymbol{U}_n(z) = \begin{pmatrix} R_a^{-\frac{1}{2}} k_n^{-1} (f_{n2,z} + f_{n1,z^3}) \\ -R_a^{-\frac{1}{2}} (f_{n2} + f_{n1,z^2}) \\ f_{n1} \\ -R_a^{-\frac{1}{2}} k_n^{-2} (\mathrm{D}^2 + k_n^2)(f_{n2,z} + f_{n1,z^3}) \end{pmatrix}. \tag{A 11}$$

We need now more information about the solutions of (A 4) at the critical Rayleigh number R_{ac}. The periodic solutions are well known (see for instance SW):

$$\beta_1 U_c(z) \mathrm{e}^{\mathrm{i}q_c x} + \text{c.c.}$$

For $R_a > R_{ac}$ the solutions with harmonic dependency in x take the form

$$\boldsymbol{U}(x,z) = \beta_1 U_1(z) \mathrm{e}^{\mathrm{i}q_1 x} + \beta_2 U_2(z) \mathrm{e}^{\mathrm{i}q_2 x} + \text{c.c.},$$

where q_1, q_2 are two wavenumbers close to q_c, and

$$q_1 = q_c + \xi_0^{-1} \epsilon^{\frac{1}{2}} + O(\epsilon), \quad q_2 = q_c - \xi_0^{-1} \epsilon^{\frac{1}{2}} + O(\epsilon),$$

$$U_1(z) = U_c(z) + \epsilon^{-\frac{1}{2}} U'_c(z) + O(\epsilon), \quad U_2(z) = U_c(z) - \epsilon^{-\frac{1}{2}} U'_c(z) + O(\epsilon).$$

ξ_0, ϵ are defined in the main text. Careful examination shows that $U_{1,2}$ vary continuously with $q_{1,2}$, which justifies the above expansion. U'_c is then defined as follows: for $R_a > R_{ac}$ we have the following solutions of (A 4):

$$[U_1(z) \mathrm{e}^{\mathrm{i}q_1 x} - U_2(z) \mathrm{e}^{\mathrm{i}q_2 x}] \epsilon^{-\frac{1}{2}}.$$

Assuming that $U_{1,2}$ are properly normalized, we get in the limit of vanishing ϵ the solution

$$\boldsymbol{U}(x,z) = U'(x,z) \mathrm{e}^{\mathrm{i}q_c x},$$

where

$$U'(x,z) = U'_c(z) + \xi_0^{-1} x U_c(z).$$

Let $\boldsymbol{F}_c$, $\boldsymbol{F}'_c$ be the vector fields of the form (A 6) related to U_c, U'_c, and

$$\boldsymbol{F}'^{+}_c = \lim_{\epsilon \to 0} (\boldsymbol{F}^{+}_1 - \boldsymbol{F}^{+}_2) \epsilon^{-\frac{1}{2}};$$

then
$$\left.\begin{aligned}(\boldsymbol{F}_{\mathrm{c}}'^{+}|\boldsymbol{F}_{\mathrm{c}}) = (\boldsymbol{F}_{\mathrm{c}}^{+}|\boldsymbol{F}_{\mathrm{c}}') = 0,\\ (\boldsymbol{F}_{\mathrm{c}}'^{+}|\boldsymbol{F}_{n}) = (\boldsymbol{F}_{n}^{+}|\boldsymbol{F}_{\mathrm{c}}') = 0.\end{aligned}\right\} \tag{A 12}$$

At $R_{\mathrm{a}} = R_{\mathrm{ac}}$ we must add $U'(x,z)$ to (A 5). We also assume that L is large enough so that exponentially growing modes can be eliminated. We keep only those modes with Re $(k_n) < 0$, and relabel them: $K_m = k_n$ for such modes. The outer solution then reads

$$\boldsymbol{U}(x,z) = \beta_1\, U_{\mathrm{c}}(z)\,\mathrm{e}^{\mathrm{i}q_{\mathrm{c}}z} + \beta_1'\, U'(x,z)\,\mathrm{e}^{\mathrm{i}q_{\mathrm{c}}z} + \sum_{n=2}^{\infty} \beta_n\, U_n(z)\,\mathrm{e}^{K_n z} + \text{c.c.} \tag{A 13}$$

We assume that the linear problem with inhomogeneous boundary conditions, i.e. (A 2)–(A 4), has at least one solution. At $R_{\mathrm{a}} = R_{\mathrm{ac}}$ any of its solutions, say $\boldsymbol{U}^{(1)}$, is the sum of an arbitrary solution of the inhomogeneous problem, say $\lambda_1\, \boldsymbol{U}_1^{(1)}$, and of solutions of the linear homogeneous problem, i.e. (A 2), (A 4) with boundary conditions

$$u = w = \theta_x = 0 \quad \text{at} \quad x = 0. \tag{A 14}$$

The linear homogeneous problem has been well studied for finite length L. It has a one-dimensional space of solutions for some $R_{\mathrm{ac}}(L)$ above R_{ac}. When removing the second boundary at $x = L$ to infinity, we want to keep only those solutions that are the limit (in some consistent sense) of solutions of the problem for finite length. Thus the half-infinite problem we consider has solutions depending on two parameters: their amplitude and their 'phase at infinity'. The solutions are then in a two-dimensional space.

Let $\boldsymbol{U}_{2,3}$ be two linearly independent solutions of this half-infinite problem. Then

$$\boldsymbol{U}^{(1)} = \lambda_1\, \boldsymbol{U}_1^{(1)} + \lambda_2\, \boldsymbol{U}_2^{(1)} + \lambda_3\, \boldsymbol{U}_3^{(1)}, \tag{A 15}$$

where $\lambda_{2,3}$ are two free real parameters. We use the scaling $\lambda_{2,3} = O(\lambda_1)$, $\boldsymbol{U}^{(1)} = O(\lambda_1)$. We need to express these solutions in the form (A 13) for the matching with the inner solution. We assumed the existence of the $\boldsymbol{U}_i^{(1)}$, and in what follows we shall assume they are given (they could be computed by numerical techniques). Let $\theta_i^{(1)}$ be the temperature perturbation associated with the above solutions. To relate it to the eigenvalue problem (A 7) we define an auxiliary vector field $\boldsymbol{\theta}_i(x,z)$:

$$\boldsymbol{\theta}_i = \begin{pmatrix} \theta_i^{(1)} \\ \theta_{i,x^2}^{(1)} \\ \theta_{i,x^4}^{(1)} \end{pmatrix}.$$

Then from (A 10)–(A 13) we have for $x_0 > 0$

$$\beta_{\mathrm{in}} = (\boldsymbol{F}_n^{+}|\boldsymbol{\theta}_i(x_0,\cdot))\,\mathrm{e}^{K_n x_0} \quad \text{for} \quad n > 1, \tag{A 16a}$$

$$\mathrm{Re}\,[(\beta_{i1} + x_0\beta_{i1}')\,\mathrm{e}^{\mathrm{i}q_{\mathrm{c}}x_0}] = (\boldsymbol{F}_{\mathrm{c}}^{+}|\boldsymbol{\theta}_i(x_0,\cdot)), \tag{A 16b}$$

$$\mathrm{Re}\,(\beta_{i1}'\,\mathrm{e}^{\mathrm{i}q_{\mathrm{c}}x_0}) = \frac{(\boldsymbol{F}_{\mathrm{c}}'^{+}|\boldsymbol{\theta}_i(x_0,\cdot))}{(\boldsymbol{F}_{\mathrm{c}}'^{+}|\boldsymbol{F}_{\mathrm{c}}')}. \tag{A 16c}$$

Applying (A 16) for a given value of x_0 leaves two free real parameters (they originate as above in the degeneracy of the linear problem). To determine these parameters, (A 16b, c) must be applied for another value of x_0. This leads through (A 13) to a solution of (A 2)–(A 4) identical with $\boldsymbol{U}_i^{(1)}$, with the β_n given by

$$\beta_n = \lambda_1\beta_{1n} + \lambda_2\beta_{2n} + \lambda_3\beta_{3n}.$$

For the asymptotic matching we shall require only the coefficient of $U_c(z)$ to be explicitly computed. In SW the β_n were computed in a different way, using a colocation method to match expansion (A 5) with the lateral boundary conditions. Although this method might be convenient for the computations, it is unclear how many free parameters are left in the resulting infinite algebraic system.

A.3. *Outer solutions of the nonlinear problem*

As $\boldsymbol{U}^{(1)}$ is a good approximation to the nonlinear problem, it can be used as the starting point of an expansion in powers of λ_1. In what follows we limit this expansion to second order. The solution of the nonlinear problem then reads:

$$\boldsymbol{U} = \boldsymbol{U}^{(1)} + \boldsymbol{U}^{(2)} + O(\lambda^3), \tag{A 17a}$$

where $\boldsymbol{U}^{(2)}$ is determined by

$$\boldsymbol{L}\boldsymbol{U}^{(2)} = \mathbf{N}(\boldsymbol{U}^{(1)}, \boldsymbol{U}^{(1)}). \tag{A 17b}$$

Applying (A 3) to (A 17a) gives the boundary condition (A 14) for $\boldsymbol{U}^{(2)}$. $\boldsymbol{U}^{(2)}$ is then determined by (A 17b) up to the addition of an arbitrary solution of the linear homogeneous problem (A 2), (A 4), (A 14).

To solve (A 17b) we insert (A 13) in its right-hand side. The computations are at this point complete analogues of those leading to the amplitude expansion (actually, $A(x)\,U_c(z)\,e^{iq_c x}$ is the leading term in the amplitude expansion), and one gets a solution $\boldsymbol{U}'^{(2)}$ of (A 17b):

$$\boldsymbol{U}'^{(2)}(x,z) = \beta_{1,1}\,U^{(2)}_{1,1}(z)\,e^{2iq_c x} + \beta_{1,-1}\,U^{(2)}_{1,-1}(z) + \text{c.c.} + \text{n.h.t.},$$

where n.h.t. stands for non-harmonic terms (i.e. linearly growing and exponential), the $U^{(2)}_{1,\pm 1}$ are to be determined from U_c only, and the coefficients are given by

$$\beta_{1,1} = \beta_1\beta_1, \quad \beta_{1,-1} = \beta_1\beta_1^*. \tag{A 18}$$

To satisfy the boundary conditions one has to add a solution $\boldsymbol{U}''^{(2)}$ of the zeroth-order linear problem (A 4) such that

$$\boldsymbol{U}^{(2)} = \boldsymbol{U}'^{(2)} + \boldsymbol{U}''^{(2)}, \quad \boldsymbol{L}\boldsymbol{U}''^{(2)} = 0, \quad \boldsymbol{U}''^{(2)}(0,z) = -\boldsymbol{U}'^{(2)}(0,z). \tag{A 19}$$

As before we have solutions of this problem in the form

$$\boldsymbol{U}''^{(2)} = \boldsymbol{U}_1''^{(2)} + \lambda_2^{(2)}\,\boldsymbol{U}_2^{(1)} + \lambda_3^{(2)}\,\boldsymbol{U}_3^{(1)}.$$

$\boldsymbol{U}_1''^{(2)}$ is a particular solution of (A 19) and $\boldsymbol{U}_2^{(1)}$, $\boldsymbol{U}_3^{(1)}$ are the above-defined solutions of (A 4)–(A 14). $\boldsymbol{U}''^{(2)}$ scales as $\boldsymbol{U}'^{(2)}$, and can be assumed to be $O(\lambda_1^2)$. From the insertion of (A 18) in (A 19) we get an expansion for $\boldsymbol{U}''^{(2)}$ in the form (A 13):

$$\boldsymbol{U}''^{(2)} = \beta_1^{(2)}\,U_c(z)\,e^{iq_c x} + \beta_1'^{(2)}\,U'(x,z)\,e^{iq_c x} + \text{n.h.t.},$$

where $\beta_1^{(2)}$, $\beta_1'^{(2)}$ are $O(\lambda_1^2)$ and can be computed from $\boldsymbol{U}''^{(2)}$ in a way similar to the β_n. However, as $\boldsymbol{U}_2^{(1)}$, $\boldsymbol{U}_3^{(1)}$ already appear at first order in (A 17a), a normalization condition must be imposed on (A 17a). To be consistent with the inner expansion we chose to impose that $\beta_1^{(2)} = 0$. This fixes $\lambda_{2,3}^{(2)}$ and hence $\beta_1'^{(2)}$.

A.4. *Matching with the amplitude expansion*

It must be noticed that the amplitude expansion is similar at its two first stages to the previous one, but involves only the harmonic and linearly growing terms in the

x-direction. Without entering into the details of its derivation, we get the amplitude expansion:

$$\boldsymbol{U}(x,z) = A(x)\,\boldsymbol{U}_c(x)\,e^{iq_c x} + \xi_0\,A_x(x)\,\boldsymbol{U}'_c(x)\,e^{iq_c x} + A^2(x)\,\boldsymbol{U}^{(2)}_{1,1}(z)\,e^{2iq_c x} + |A^2(x)|\,\boldsymbol{U}^{(2)}_{1,-1}(z) + O(A^3) + O(AA_x) + O(\epsilon A). \quad \text{(A 20)}$$

Notice that, near the boundary, A scales like λ_1 and, if $\lambda_1 \gg \epsilon^{\frac{1}{2}}$, A_x scales like λ_1^2 (see the boundary solution (15) in the main text). Matching the 'outer' expansion with (A 20) gives

$$A(0) = \sum_{i=0}^{3} \lambda_i \beta_{i1} + O(\lambda_i^3), \quad A_x(0) = \sum_{i=0}^{3} \lambda_i \beta'_{i1} + \beta'^{(2)}_1 + O(\lambda_i^3). \quad \text{(A 21)}$$

Matching the higher-order terms in (A 20) gives expressions consistent with (A 18). From (A 21) the parameters λ_2, λ_3 can be eliminated, yielding the boundary conditions:

$$A + \xi_1 A_x + \xi_2 A_x^* = \lambda\,e^{i\phi_0} + O(\lambda^2)$$

at $x = 0$, where λ, ϕ_0, ξ_1, ξ_2 are some real coefficients, and $\lambda = O(\lambda_1)$. For $\lambda_1 = O(\epsilon^{\frac{1}{2}})$ one gets at first order:

$$A(0) = \lambda\,e^{i\phi_0} + O(\lambda^2).$$

If $\lambda_1 = O(\epsilon)$ the inner expansion gives $A_x = O(\epsilon)$, and the boundary condition is

$$A + \xi_1 A_x + \xi_2 A_x^* = \lambda\,e^{i\phi_0} + O(\epsilon^2). \quad \text{(A 22)}$$

As symmetrical boundary conditions are imposed at $x = L$ (A 3), this results in identical boundary conditions for $A\,e^{iq_c(L-x)}$, as can be seen from the definition of A:

$$A(L) = \lambda\,e^{i(q_c L - \phi_0)}.$$

The phase difference $\Delta\phi$ across the interval $(-L, L)$ defined in the main text is then

$$\Delta\phi = 2q_c L - 2\phi_0. \quad \text{(A 23)}$$

Appendix B. Wavenumber selection for small boundary forcing

We consider the case where the forcing is small, i.e. $\lambda \ll \epsilon^{\frac{1}{2}}$. The proposed method is new and applicable also for $\lambda = 0$. Our starting point for investigating wavenumber selection is the second-order stationary amplitude equation. Such an equation can be derived under the same assumptions as the first-order amplitude equation (1). It cannot be made two-dimensional in many problems, owing to non-local contributions (Siggia & Zippelius 1981). However, we are not bothered by this problem for the 1-dimensional amplitude equation. This stationary amplitude equation is

$$\epsilon A + \xi_0^2 A_{xx} - \frac{|A|^2 A}{A_0^2} + ig_1\,\epsilon A_x + ig_2\,|A|^2 A_x + ig_3\,A_x^* A^2 = 0. \quad \text{(B 1)}$$

We consider this equation together with the boundary conditions (A 22). Terms of the form $|A|^4$ are excluded by symmetry arguments: (B 1) should be invariant under the change $A \to -A$. The absence of terms of the form A_{x^3} needs some explanation. A trivial way to derive an amplitude equation $O(\epsilon^2)$ is to take the derivative of (1). Thus there are actually two equations $O(\epsilon^2)$ and they can be suitably combined to give (B 1). Further, the absence of the A_{x^3}-term allows compatibility with the number of boundary conditions: one condition at every boundary fits a second-order differential equation, not a third-order one.

Multiplying (B 1) by $-\mathrm{i}A^*$ and adding the complex conjugate leads to an expression of the form

$$\frac{\mathrm{d}K_1}{\mathrm{d}x} = 0,$$

where $$K_1 = \tfrac{1}{2}\mathrm{i}\xi_0^2(AA_x^* - A^*A_x) + \tfrac{1}{4}(g_2+g_3)|A|^4 + \tfrac{1}{2}g_1\epsilon|A|^2. \tag{B 2}$$

K_1 is related to the invariant K of (1):

$$\mathrm{i}\xi_0^2 K = K_1 + O(\epsilon^2).$$

Multiplying (B 1) by A and adding the c.c. leads to

$$\frac{\mathrm{d}E_1}{\mathrm{d}x} = \mathrm{i}g_3 A_{xx}^* A|A|^2 + \text{c.c.}, \tag{B 3}$$

where $$E_1 = \tfrac{1}{2}\epsilon|A|^2 - \frac{1}{4}\frac{|A|^4}{A_0^2} + \tfrac{1}{2}\xi_0^2|A_x|^2 + \tfrac{1}{2}\mathrm{i}g_3(AA_x^* - A^*A_x)|A|^2.$$

However, from (1),

$$A_{xx} = \xi_0^{-2}\left(-\epsilon A + \frac{|A|^2 A}{A_0^2}\right) + O(\epsilon^2).$$

By substituting in (B 3), one gets at the relevant order

$$\frac{\mathrm{d}E_1}{\mathrm{d}x} = 0. \tag{B 4}$$

K_1 and E_1 can be estimated easily away from the boundaries, using (2) and assuming $\delta \ll \epsilon^{\frac{1}{2}}$:

$$K_1 = A_0^2\epsilon\{\xi_0^2\delta + \tfrac{1}{4}[(g_2+g_3)A_0^2\epsilon + 2g_1\epsilon]\} + O(\epsilon^3). \tag{B 5a}$$

$$E_1 = \tfrac{1}{4}\epsilon^2 A_0^2. \tag{B 5b}$$

Estimation of K_1 on the boundary is slightly more subtle. As shown in Appendix A, two parameters remain free at the boundary. We choose them to be

$$c = |A_x(0)|, \quad \theta = \arg(A_x(0)).$$

As $|A(0)| \ll \epsilon^{\frac{1}{2}}$, the estimation of $E_1|_b$ is easy:

$$E_1|_b = \tfrac{1}{2}\xi_0^2 c^2.$$

Equating with (B 5b) gives finally

$$A_x(0) = \frac{A_0\epsilon}{\sqrt{2}\,\xi_0}\mathrm{e}^{\mathrm{i}\theta}. \tag{B 6}$$

Replacing in (A 22) gives

$$A(0) = \lambda\,\mathrm{e}^{\mathrm{i}\phi_0} - \frac{A_0}{\sqrt{2}\,\xi_0}(\xi_1\,\mathrm{e}^{\mathrm{i}\theta} + \xi_2\,\mathrm{e}^{-\mathrm{i}\theta}).$$

From (B 2)

$$K_1|_b = A_0^2\epsilon^2\left(\frac{\lambda\xi_0}{\sqrt{2}\,A_0\epsilon}\sin(\phi_0-\theta) - \tfrac{1}{2}(\xi_{1\mathrm{i}} + \xi_{2\mathrm{r}}\sin 2\theta - \xi_{2\mathrm{i}}\cos 2\theta)\right) \tag{B 7}$$

where $$\xi_j = \xi_{j\mathrm{r}} + \mathrm{i}\xi_{j\mathrm{i}} \quad \text{for } j = 1, 2.$$

Equating (B 5a) and (B 7) gives

$$\delta = \frac{\lambda\xi_0^{-1}}{\sqrt{2}\,A_0}\sin(\phi_0-\theta) - \tfrac{1}{2}(\xi_{1\mathrm{i}} - \xi_{2\mathrm{r}}\sin 2\theta + \xi_{2\mathrm{i}}\cos 2\theta)\epsilon\xi_0^{-2} - (2g_1\epsilon + (g_2+g_3)A_0^2\epsilon)/4\xi_0^2. \tag{B 8}$$

From (B 8), the precise bounds for δ can be derived, knowing all the constants g_j, ξ_j, λ, ϕ_0, A_0 and ϵ. (In the general case, this requires the resolution of a fourth-order algebraic equation.) Moreover, δ is a periodic function of θ with period 2π. For $\lambda \ll \epsilon$ this can be observed as a slight splitting in two of the extrema for δ, as obtained when scanning the set of stable modes.

We now apply those results to the following model, introduced by Lange & Newell (1971):

$$\psi_{tt} = \epsilon\psi - \left(\frac{\mathrm{d}^2}{\mathrm{d}x^2} + q_0^2\right)^2 \psi - \psi^3.$$

Stationary solutions are investigated with boundary conditions modelling inhomogeneous forcing, i.e.

$$\psi_x = \lambda, \quad \psi = 0 \quad \text{for } x = \pm L.$$

The boundary conditions on the slowly varying amplitude are then

$$\left.\begin{aligned} \operatorname{Re} A &= 0, \\ q_0 \operatorname{Im} A + \operatorname{Re} A_x &= \lambda \end{aligned}\right\} \quad \text{for } x = \pm L,$$

or else

$$A - \frac{\mathrm{i}}{2q_0}(A_x + A_x^*) = \frac{\mathrm{i}\lambda}{q_0} \quad \text{for } x = \pm L.$$

The stationary amplitude equation is easy to derive, owing to the simplicity of the nonlinear term in the above model:

$$\epsilon A + 4q_0^2 A_{xx} - \tfrac{3}{4}|A|^2 A - \mathrm{i}\epsilon A_x + \tfrac{3}{2}\mathrm{i}|A|^2 A_x + \tfrac{3}{4}\mathrm{i}A_x^* A^2 = 0.$$

There results

$$K = \tfrac{1}{3}\epsilon(\epsilon q_0^{-1} + 16q_0^2\delta), \quad K_b = \tfrac{2}{3}(\lambda q_0 \epsilon \sqrt{6}\cos\theta + q_0^{-1}\epsilon^2\cos^2\theta),$$
$$\delta_- < \delta < \delta_+,$$

with

$$\delta_- = \inf\left(-\frac{\epsilon}{16q_0^3}, \frac{\epsilon}{16q_0^3} - \frac{\lambda\sqrt{6}}{8q_0}\right), \quad \delta_+ = \frac{\epsilon}{16q_0^3} + \frac{\lambda\sqrt{6}}{8q_0}.$$

These results are plotted on figure 3.

Appendix C. Computation of finite-length solutions

The integral (13a) can be rewritten in the form

$$l = 2^{\frac{1}{2}} \int_{r_m}^{b} \frac{r\,\mathrm{d}r}{(\frac{1}{2}r^6 + 2Er^2 - r^4 - K^2)^{\frac{1}{2}}}, \tag{C 1}$$

where

$$K = (1-a^2)\,a, \quad E = \tfrac{1}{2}(1-a^2)(1+3a^2) + \eta.$$

The denominator in (C 1) has the roots

$$r_{1\pm} = (1-a^2)^{\frac{1}{2}} \pm \frac{\eta^{\frac{1}{2}}}{1-3a^2} + O(\eta),$$

$$r_2 = \sqrt{2}\,a - \frac{2\sqrt{2}\,a}{1-3a^2}\eta,$$

$$r'_{1\pm} = -r_{1\pm}, \quad r'_2 = -r_2.$$

For $\eta > 0$ and at lowest order in η this integral can be expressed as

$$l = 2^{-\frac{1}{2}} \int_{r_m^2}^{b^2} \frac{\mathrm{d}u}{(u-2a^2)^{\frac{1}{2}}[(u-a^2+1)^2+\eta(1-3a^2)^{-2}]^{\frac{1}{2}}}. \tag{C 2}$$

Moreover, as $r_x = 0$ for $r = r_m$, r_m is a root of the denominator. Examination of motion in the potential V (figure 5*b*) gives $r_m = r_2$. The leading contribution to (C 2) comes for $u \simeq 1-a^2$. Integrating in this region gives

$$l = \frac{2^{-\frac{1}{2}}}{(1-3a^2)^{\frac{1}{2}}} \operatorname{Log} \frac{\eta(1-a^2)^2}{1-3a^2}.$$

For $\eta < 0$, $r_m = r_{1+}$, and we get in a similar way

$$l = 2^{-\frac{3}{2}}(1-3a^2)^{-\frac{1}{2}} \operatorname{Log} \frac{\eta(1-a^2)^2}{1-3a^2}.$$

To compute (13*b*), we extract from $\Delta\phi$ its bulk part, proportional to al. There results

$$\Delta\phi - al = I(a, b, \eta),$$

where

$$I(a, b, \eta) = 2^{-\frac{1}{2}} \int_{r_m^2}^{b^2} \frac{-a(u-u_1)\,\mathrm{d}u}{u(u-u_2)^{\frac{1}{2}}[(u-u_1)^2+\alpha^2\eta]^{\frac{1}{2}}}.$$

The main contribution to the integral is now outside the region $u \approx u_1$, and

$$\begin{aligned} I(a, b, \eta) &= -2^{-\frac{1}{2}} \int_{r_m^2}^{b^2} \operatorname{sgn}(u-u_1) \frac{a\,\mathrm{d}u}{u(u-u_2)^{\frac{1}{2}}} + O(\eta) \\ &= 2F(u_1) - F(b^2) - F(r_m^2), \end{aligned}$$

where

$$F(y) = \frac{a}{u_2^{\frac{1}{2}}} \arctan \frac{(y-u_2)^{\frac{1}{2}}}{u_2^{\frac{1}{2}}}.$$

According to the sign of η, $r_m^2 = u_2$ or u_1, which gives (14) in the main text.

REFERENCES

Abramowitz, M. & Stegun, I. A. 1968 *Handbook of Mathematical Functions*, p. 17. Dover.

Benjamin, T. B. 1978*a* *Proc. R. Soc. Lond.* A **359**, 1.

Benjamin, T. B. 1978*b* *Proc. R. Soc. Lond.* A **359**, 27.

Boucif, M., Wesfreid, J. E. & Guyon, E. 1983 to be published.

Croquette, V. & Pocheau, A. 1984 In *Cellular Structures in Instabilities* (ed. J. E. Wesfreid & S. Zaleski). Springer.

Cross, M. C., Daniels, P. G., Hohenberg, P. C. & Siggia, E. D. 1983*a* *J. Fluid Mech.* **127**, 155.

Cross, M. C., Hohenberg, P. C. & Lücke, M. 1983*b* *J. Fluid Mech.* **136**, 269.

Daniels, P. G. 1977 *Proc. R. Soc. Lond.* A **378**, 173.

Daniels, P. G. 1978 *Mathematika* **25**, 216.

Daniels, P. G. 1981 *Proc. R. Soc. Lond.* A **378**, 539.

Eckhaus, W. 1965 *Studies in Non Linear Stability Theory*. Springer.

Graham, R. W. & Domaradzki, J. A. 1982 *Phys. Rev.* A **26**, 1572.

Hall, P. & Walton, I. C. 1977 *Proc. R. Soc. Lond.* A **358**, 199.

Kogelman, S. & DiPrima, R. C. 1970 *Phys. Fluids* **13**, 1.

Kramer, L. & Hohenberg, P. C. 1984 In *Cellular Structures in Instabilities* (ed. J. E. Wesfreid & S. Zaleski). Springer.

LANGE, X. & NEWELL, A. C. 1971 *SIAM J. Appl. Maths* **21**, 603.

MULLIN, T. 1982 *J. Fluid Mech.* **121**, 207.

NEWELL, A. C. & WHITEHEAD, J. A. 1969 *J. Fluid Mech.* **38**, 279.

NORMAND, C. 1984 *J. Fluid Mech.* **143**, 223.

PFISTER, G. & REHBERG, I. 1981 *Phys. Lett.* **83A**, 19.

POMEAU, Y. & ZALESKI, S. 1981 *J. Phys.* (*Paris*) **42**, 515.

POMEAU, Y., ZALESKI, S. & MANNEVILLE, P. 1983 *Phys. Rev.* A **27**, 2710.

POTIER FERRY, M. 1983 In *Collapse: The Buckling of Structures in Theory and Practice* (ed. J. M. T. Thomson & G. W. Hunt). Cambridge University Press.

SCHAEFFER, D. G. 1980 *Math. Proc. Camb. Phil. Soc.* **87**, 307.

SEGEL, L. A. 1969 *J. Fluid Mech.* **38**, 203.

SIGGIA, E. D. & ZIPPELIUS, A. 1981 *Phys. Rev. Lett.* **47**, 835.

SNYDER, H. A. 1969 *J. Fluid Mech.* **35**, 273.

STEWARTSON, K. & WEINSTEIN, M. 1979 *Phys. Fluids* **22**, 1421.

WALTON, I. C. 1980 *Proc. R. Soc. Lond.* A **372**, 201.

WESFREID, J. E., BERGE, P. & DUBOIS, M. 1979 *Phys. Rev.* A **19**, 1231.

WESFREID, J. E. & CROQUETTE, V. 1980 *Phys. Rev. Lett.* **45**, 634.

WESFREID, J. E., POMEAU, Y., DUBOIS, M., NORMAND, C. & BERGE, P. 1978 *J. Phys. Lett.* (*Paris*) **39**, 725.

ZALESKI, S. 1984 In *Cellular Structures in Instabilities* (ed. J. E. Wesfreid & S. Zaleski). Springer.